European Polymer Journal

Surface wetting driven release of antifibrotic Mitomycin-C drug from modified biopolymer thin films

--Manuscript Draft--

Manuscript Number:	EUROPOL-D-20-00154R1
Article Type:	Research paper
Section/Category:	Regular Paper
Keywords:	mitomycin; biopolymer layer; Surface modification; adjusted surface wetting; Drug release
Corresponding Author:	Laszlo Janovak, PhD University of Szeged Szeged, -- Select a State (only if United States or Canada HUNGARY
First Author:	Tamás Takács
Order of Authors:	Tamás Takács
	Mohamed M. Abdelghafour
	Ágota Deák
	Diána Szabó
	Dániel Sebők, PhD
	Imre Dékány
	László Rovó
	Ákos Kukovecz
	Laszlo Janovak
Abstract:	We demonstrate that Nature-inspired lotus-like non-wetting phenomena can also be used in the field of controlled drug delivery. Hydrophobically modified, and cellulose microparticle-roughened polyvinyl alcohol (PVA) biopolymer based thin films were synthetised and converted into superhydrophobic (Θ=165.3°; [[EQUATION]] = 1.7±0.67 mJ/m 2) thin films. The surface wetting of the thin films was adjustable from superhydrophilic to superhydrophobic nature and this affected the drug release properties as well. We also prove that this surface wetting driven drug delivery system (DDS) is suitable for the encapsulation and prolonged/ adjusted release of Mitomycin (MMC), a drug with antifibrotic properties. The in vitro release experiments conducted under physiological conditions (PBS, pH = 7.4) revealed that –due to the lower crystallinity– the release of MMC was faster (k'=6.1×10 -6 mM/s) from the hydrophilic film compared to the pure, crystalline (k'=1.21×10 -6 mM/s) MMC. Neverteless, significantly lower MMC dissolution rate (k'=5×10 -8 mM/s) was obtained for the superhydrophobic sample featuring a non-wetting, lotus-like nature. Based on this in vitro study, we suggest that the presented surface wetting driven DDS loaded with MMC could be useful for example in the area of head and neck surgeries to prevent scar tissue formation.
Suggested Reviewers:	Vera Constantino, PhD Departamento de Química Fundamental, Instituto de Química, Universidade de São vrlconst@iq.usp.br expert in organic/ inorganic drug releasing systems
	Andrew Swift, PhD University of Liverpool haroneswift@yahoo.co.uk Nasal application experience of mitomycin
	Maria Rosa Aguilar de Armas, PhD Institute of Polymer Science and Technology (ICTP-CSIC), Spain mraguilar@ictp.csic.es

Surface wetting driven release of antifibrotic Mitomycin-C drug from modified biopolymer thin films

Tamás Takács[1,2], Mohamed M. Abdelghafour[1,3,] Ágota Deák[1], Diána Szabó[4], Imre Dékány[1], László Rovó[4], Ákos Kukovecz[2,*], László Janovák[1*]

[1]*University of Szeged, Interdisciplinary Excellence Centre, Department of Physical Chemistry and Materials Science, H-6720, Rerrich Béla tér 1, Szeged, Hungary*

[2]*University of Szeged, Interdisciplinary Excellence Centre, Department of Applied and Environmental Chemistry, H-6720, Rerrich Béla tér 1, Szeged, Hungary*

[3]*Department of Chemistry, Faculty of Science, Zagazig University, Zagazig 44519, Egypt*

[4]*Department of Oto-Rhino-Laryngology and Head & Neck Surgery, University of Szeged, H-6724, Tisza Lajos krt. 111, Szeged, Hungary*

Graphical abstract:

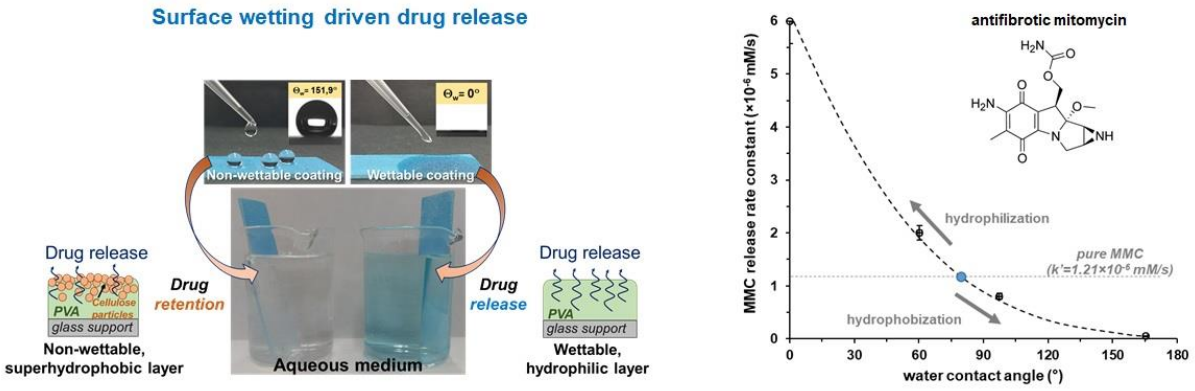

Surface wetting driven release of antifibrotic Mitomycin-C drug from modified biopolymer thin films

Tamás Takács[1,2], Mohamed M. Abdelghafour[1,3,] Ágota Deák[1], Diána Szabó[4], Dániel Sebők[2], Imre Dékány[1], László Rovó[4], Ákos Kukovecz[2,*], László Janovák[1*]

[1]*University of Szeged, Interdisciplinary Excellence Centre, Department of Physical Chemistry and Materials Science, H-6720, Rerrich Béla tér 1, Szeged, Hungary*

[2]*University of Szeged, Interdisciplinary Excellence Centre, Department of Applied and Environmental Chemistry, H-6720, Rerrich Béla tér 1, Szeged, Hungary*

[3]*Department of Chemistry, Faculty of Science, Zagazig University, Zagazig 44519, Egypt*

[4]*Department of Oto-Rhino-Laryngology and Head & Neck Surgery, University of Szeged, H-6724, Tisza Lajos krt. 111, Szeged, Hungary*

[*] Corresponding authors. Tel.: +36 62 544 210; Fax: +36 62 544 042.

E-mail address: janovakl@chem.u-szeged.hu (L. Janovák)

E-mail address: kakos@chem.u-szeged.hu (Á. Kukovecz)

Abstract

We demonstrate that Nature-inspired lotus-like non-wetting phenomena can also be used in the field of controlled drug delivery. Hydrophobically modified, and cellulose microparticle roughened polyvinyl alcohol (PVA) biopolymer based thin films were synthetised and converted into superhydrophobic (Θ=165.3°; γ_s^{tot} = 1.7±0.67 mJ/m^2) thin films. The surface wetting of the thin films was adjustable from superhydrophilic to superhydrophobic nature and this affected the drug release properties as well.

We also prove that this surface wetting driven drug delivery system (DDS) is suitable for the encapsulation and prolonged/ adjusted release of Mitomycin (MMC), a drug with antifibrotic properties. The *in vitro* release experiments conducted under physiological conditions (PBS, pH = 7.4) revealed that –due to the lower crystallinity– the release of MMC was faster (k'=6.1×10^{-6} mM/s) from the hydrophilic film compared to the pure, crystalline (k'=1.21×10^{-6} mM/s) MMC. Neverteless, significantly lower MMC dissolution rate (k'=5×10^{-8} mM/s) was obtained for the superhydrophobic sample featuring a non-wetting, lotus-like

nature. Based on this *in vitro* study, we suggest that the presented surface wetting driven DDS loaded with MMC could be useful for example in the area of head and neck surgeries to prevent scar tissue formation.

Keywords: mitomycin, biopolymer layer, surface modification, adjusted surface wetting, drug release

1. Introduction

Mitomycin C (MMC) isolated from *Streptomyces caespitosus* is an antineoplastic, antifibrotic [1] and antibiotic, poorly water soluble anti-proliferative bifunctional alkylating agent which causes the inhibition of the DNA-synthesis by bonding to the DNA chains [2,3]. Apart from the administration as a commonly known chemotherapeutic agent, MMC is widely used as an antifibrotic drug after ophthalmic and – nowadays more and more often – after head and neck surgeries to prevent scar tissue formation [4,5]. Although MMC is soluble in water, its reported solubility and thus its bioavailability is very low (~0.9 mg/mL) [6]. Thus, it is essential to make efforts to improve its utility by reducing its size to micro- or nano level and improve drug efficacy and bioavailability by using various delivery methods. The intermolecular forces of attraction in dissolving a solute can be reduced in order to improve the solubility of a drug [7]. Ethanol is one of the typical organic solvents highly miscible with water, also it is classified in Class 3 of ICH guidelines and residual ethanol in finished product has a low safety risk [8]. The increased solubility with the addition of ethanol is most likely due to the formation of hydration shell around the MMC that acts as a compatible layer between the drug and ethanol [9].

MMC administered in a free form (e.g. subcutaneous injection) is excreted from the body in a very short period of time [10]. Therefore, in order to provide the prolonged therapeutic effect of the drug, it is required to design and apply drug delivery systems (DDS) which are capable of prolonged drug release. Biocompatible, polymer-based (e.g. polyvinyl alcohol/cellulose) composite drug delivery systems allow targeted, prolonged, effective localised drug release without systemic side effects or harm to other organs. Other advantage of DDS is that they can be modified [11] to fulfill the requirements of the drug administration, treatment conditions, area of application, the needs of the patient, thus, achieving the maximal therapeutic effect.

Since polyvinyl alcohol (PVA) is a biocompatible, biodegradable synthetic polymer, which has good mechanical properties and is easy to modify, provides an excellent basis for DDS. Thanks

to the characteristics mentioned above PVA displays mucoadhesive/bioadhesive properties which can be exploited during the process of drug release. Mucoadhesive drug delivery systems have many advantages over the conventional drug delivery systems: they increase the contact time between the drug and the biological substrate which facilitates drug absorption and by attaching to the specific sites of the body they enhance the bioavailability of the drug [12,13]. Besides its biomedical applications (e.g. drug delivery devices, contact lenses, wound dressings promoting wound healing), PVA plays a significant role in electronics [14], cosmetics (e.g. skin- and body care) [15] and it is also frequently used for tissue engineering purposes, such as fabrication of artificial cartilage, vascular and bone tissue, etc. [16–22]. The silane-modified or hydrophobized polyvinyl alcohols have the same scope of application as non-derivatized polyvinyl alcohols. Thus, they are applied in cosmetics, especially hair cosmetics as well as in food packaging [23] and they can be also used to fabricate DDS displaying (super)hydrophobic properties [24]. Cellulose is one of the most abundant biopolymers on Earth. As a biocompatible material having excellent mechanical properties, cellulose is widely used in different fields depending on the particle size, shape and degree of crystallinity, such as cosmetics (e.g. stabilizer, thickener), food (e.g. adjuvant) and pharmaceutical industries (e.g. binder), and biomedical field (e.g. extended drug release in drug delivery systems) [25–27].

The rate of the drug release from the polymer network can be tuned by modifying the physico-chemical properties (hydrophobicity, pore and particle size, etc.) of the DDS, such as preparing superhyrophobic surfaces by changing the wettability of the polymer network, e.g. by surface functionalization or by surface roughening [28,29]. Conducting the drug release experiment and fitting the appropriate kinetic model (e.g. zero, first or second order kinetics, Korsmeyer-Peppas, Hopfenberg model, Higuchi's, Weibull's equation, etc.) to the obtained set of data points, it is possible to get an insight into the mechanism of the drug release (as well as to come up with new methods to develop our DDS) [30,31].

Numerous surfaces, e.g. leaves of certain plant species, the wings of butterflies and related insects, found in nature, exhibit superhydrophobic properties, thus, they are said to possess so called self-cleaning ability [32–34]. The wettability of a surface is determined by its roughness, chemical composition or surface topography. Hydrophobic surfaces which have roughness on the micro- and/or nanometer scale show superhydrophobic properties [35,36]. The relation between surface roughness and wettability first described by Wenzel [37], Cassie and Baxter [38] provided a valuable basis for further research [35]. Non-wettable surfaces having high water contact angles (WCAs> 150°) and high droplet mobility even at a small tilt angle, are called superhydrophobic surfaces [34,39]. Increasing the roughness of non-wettable surfaces

increases their water-repellency and leads to higher water contact angles. The adhesive interactions between the water droplets and the surface are getting stronger with greater roughness as it increases the contact area between them. However, when the roughness reaches a critical value, it is energetically more favourable for the water droplets to bridge over the roughness. At great roughness values the contact area between the droplets and the surface is decreased, thus, it rolls off the surface easily, carrying away any contamination [36,40]. The operational principle of self-cleaning surfaces, described above, laid the basis for designing our drug delivery systems.

This paper reports about the designing, testing and characterization of surface wetting driven drug delivery systems (DDS) suitable for the encapsulation and prolonged release of MMC. The *in vitro* release experiments were conducted under physiological conditions (PBS, pH = 7.4) with DDS having different surface properties (such as different roughness and wettability). It was found out that the rate of MMC drug release can be tuned by changing the wettability of the system's surface.

2. Materials and methods

Materials

For the synthesis of biopolymer thin films polyvinyl alcohol (PVA, degree of hydrolysis: 86 – 89%) was acquired from Nagart Kft., Hungary. Cellulose powder (0.02–0.15 mm, acid washed) and microcrystalline cellulose (20 μm) were acquired from Fluka and from Sigma-Aldrich, respectively. The MMC ($C_{15}H_{18}N_4O_5$, 10 mg) as model drug was purchased from Medac GmbH, Wedel, Germany. For the preparation of phosphate buffered saline solution (pH = 7.4) disodium hydrogen phosphate dodecahydrate ($Na_2HPO_4 \times 12H_2O$) and sodium chloride (NaCl) were obtained from Molar Chemicals Kft., Hungary, while sodium dihydrogen phosphate monohydrate ($NaH_2PO_4 \times H_2O$) from Sigma-Aldrich. Butyl trichlorosilane (≥98 %) was purchased from Sigma–Aldrich. All chemicals were used as received without further purification.

2.1. Hydrophobization of water-soluble PVA biopolymer with butyl trichlorosilane

Functionalization of PVA with butyl trichlorosilane (BTS) was performed according to the following protocol: 0.5 g of PVA powder was dispersed in 10 mL of hexane solution with a systematically varied volume ratio of BTS silylating agent (0, 0.01, 0.1, 0.25, 0.5, 1, 2 and 5 v/v%). The reaction mixture was left under magnetic stirring for 1.5 h at room temperature until

the completion of the silylation reaction. After the reaction time, the dispersion was decantated and the BTS-PVA product was washed two times with hexane to remove residue of silylating agent followed by leaving in the oven at 50 ^{o}C for 30 min to remove the excess of solvent. A water dispersibility test was applied to check the hydrophobization and wetting of the obtained products.

2.2. Preparation of thin films

2.2.1. Preparation of MMC loaded PVA based thin films

The PVA thin films containing MMC were prepared by the solvent casting process. First, the PVA or hydrophobized BTS-PVA was dissolved in water/ethanol (=90/10 v/v%) mixture to get a 10 wt.% homogeneous polymer solution and afterwards 1.5625 mg MMC powder was dissolved in 6.25 g of this solution. Next, the prepared solution containing both the MMC and PVA was subjected to ultrasound for 1 minute to ensure homogeneous composition. Lastly, the homogeneous MMC/PVA solution was transferred into a petri dish, followed by drying in an oven for 24 hours at 60 °C. Accordingly, the final thin (60.8±5.5 μm) film contains 0.25 wt.% MMC.

2.2.2. Preparation of MMC loaded and cellulose roughened PVA thin films

Cellulose microparticles roughened thin films were also prepared using the same synthesis method. Before the preparation, a cellulose mixture was prepared consisting of 1:1 weight ratio of cellulose powder (0.02–0.15 mm) and microcrystalline cellulose (20 μm). During the film synthesis 6 × 1.5625 mg MMC powder was dissolved in 10.00, 7.50, 5.00, 2.50, 1.25, 0.626 g of 5 wt.% PVA solution, respectively. Next 0.1250, 0.2500, 0.3750, 0.5000, 0.5625, 0.5938 g of cellulose powder mixture was added to this solution to get samples with increasing (19.95, 39.90, 59.85, 79.80, 89.78 and 94.76 wt.%, respectively) cellulose content (**Table 1.**).

In the following step, the prepared suspension was subjected to ultrasound for 1 minute to ensure homogeneous composition. Lastly, the homogeneous MMC/cellulose/PVA suspension was dried in an oven for 24 hours at 60 °C. Both hydrophilic and hydrophobic MMC loaded, cellulose roughened PVA thin film series were prepared. Beside the 0.25 wt.% MMC containing samples MMC free PVA based thin films were also synthtised for references.

Table 1. Mass of the added components during the synthesis and the measured film thickness and porosity values.

Cellulose content (wt.%)	**19.95**	**39.9**	**59.85**	**79.8**	**89.78**	**94.76**
5 wt.% PVA solution (g)	10	7.5	5	2.5	1.25	0.625
Cellulose powder mixture (g)	0.125	0.25	0.375	0.5	0.5625	0.5938
MMC powder (g)	$1.5625 \cdot 10^{-3}$					
Film thickness (μm)	60.8±5.5	98.3±6.4	149.9±8.9	174.8±7.5	193.2±9.5	206.6±10.2
Porosity (%)*	24.1±2.3	41.5±3.9	64.9±3.7	72.3±3.8	76.5±4.7	77.3±6.5

* from CT measurements

2.3. Methods of characterization

The solubility of the polymers in water and water/ethanol (=90/10 v/v.%) mixture was studied by gravimetric analysis. The initial PVA and BTS hydrophobized PVA samples were dispersed/ dissolved in the solvents in a concentration of 15 wt.% and the samples were continuously stirred for 48 hours. Next, the samples were centrifuged (5000 rpm, 5 min), the supernatant (polymer solutions) were decanted and the remaining sediments (undissolved polymer particles) were dried (60°C for overnight) and weighed.

The Fourier Transform Infrared Spectroscopy (FTIR) measurements were performed on the BTS-modified PVA biopolymer applying a BioRad FTS-60A FT-IR spectrometer. The spectra were registered between 3600 and 600 cm^{-1} at a resolution of 2 cm^{-1}.

The quantitative determination of OH value was evaluated via an acetic anhydride/pyridine titration method. The acetylating agent was prepared by using 1.5 mL of acetic anhydride and 28.5 mL of pyridine with volume ratio (1:19). This solution was stirred for 1 h before usage. Next, 0.1 g of PVA with different BTS hydrophobization percent (0, 0.01, 0.1, 0.25, 0.5, 1, 2 and 5 v/v%, respectively) was put in 5 mL of acetylating agent and the reaction mixture was stirred at 65 ^{o}C for 24 h. After the reaction time, 5 mL distilled water was added to convert the excessive acetic anhydride into acetic acid, which was titrated by 0.2 M NaOH in the presence of phenolphthalein solution (1% w/v in ethanol) as an indicator. Blank solutions without PVA were also tested as a control. The hydroxyl value (I_{OH}) was calculated using Equation (1):

$$I_{OH} = \frac{(B-S) \cdot N \cdot 40}{W} \qquad (1)$$

where B and S are the volumes in mL of NaOH solution consumed by the blank and sample, N is the normality of the NaOH solution (0.2 M) and W is the sample weight (g) added to the acetylation.

The water content of hydrogel was investigated by using thermogravimetric (TG) analysis. The sample was prepared by adding 50 mg of polymer to 1 mL of distilled water and stirred for 48 h to reach equilibrium. After a time, the samples were centrifuged and the precipitate was measured by TG. During TG measurements, the samples were heated from 25-200 °C with a heating rate of 5 °C/min (Mettler-Toledo TGA/SDTA 851e Instrument).

The surface structure and morphology of the prepared thin film samples were examined applying a field emission scanning electronmicroscope (SEM−Hitachi S-4700) using a secondary electron detector and 10 kV acceleration voltage, while the presence of the drug, *i.e.* the nitrogent content of the MMC in the thin films were studied using a Röntec EDX detector.

Profilometry measurements were performed using a Veeco, Dektak 8 Advanced Development Profiler®. The tips employed had a radius of curvature of 5 μm, and the force applied to the surface during scanning was ~30 μN. The length examined was 1000 μm for each sample. The measurement range was 655 kÅ and the resolution was 0.167 μm/sample. The used short and long pass filter cutoff were 25–25 μm. The data have been evaluated by Dektak software (Microsoft® Windows XP®: interactive data acquisition).

The inner structure and porosity of the initial PVA film and cellulose containing (super)hydrophobic layer were investigated via X-ray micro-computed tomography analysis, which was conducted using the X-ray Microtomography equipment (Bruker Skyscan 2211, Belgium). The samples were scanned using 11Mp cooled CCD camera by applying the source voltage of 60 kV and the source current 500 μA with an exposure time of 550 ms. The voxel size of these dataset was 800x800x800 nm^3. NRecon reconstruction software was used to reconstruct the projected images with the pixel size of 4032 x 2688 and CTVox and CTAn (Bruker, Belgium) software were used to represent the 3D models and the 2D cross sections, respectively.

The thickness of the films was measured using an Elcometer 224 type digital profile gauge.

The initial contact angles on the cellulose particles roughened films were measured according to the sessile drop technique at 25.0± 0.5 °C under atmospheric pressure, applying an EasyDrop drop shape analysis system (Krüss GmbH, Hamburg, Germany) equipped with DSA100 software, a Peltier temperature chamber and a steel syringe needle of 0.5 mm diameter and using distilled water as a test liquid.

The advancing and receding contact angles were also measured according to the protocol of Drelich [41]. The obtained advancing and receding contact angles are also suitable for the estimation of the total apparent surface free energy (γ_s^{tot}) of the layer, knowing the surface tension of the probe liquid, (γ_l, 72.1 mN/m in the case of distilled water at 25°C) and its contact angle hysteresis, which is defined as the difference between the advancing (Θ_a) and receding (Θ_r) contact angles (2) [42]:

$$\gamma_s^{tot} = \left(\frac{\gamma_1(1+\cos\theta_a)^2}{(2+\cos\theta_r+\cos\theta_a)}\right) \qquad (2)$$

Beside the above presented total surface free energy determination method, the polar and dispersive components were also determined by contact angle measurements. Overall surface free energy (γ_s^{tot}) and its polar (γ_s^P) and dispersive (γ_s^D) components of the composites with increasing cellulose loading were determined from seven sets of contact angles using different test liquids with different surface free tension values (**Table S1**.) according to Owens-Wendt-Kaelble equation ([43]).

$$\gamma_1(1 + \cos\Theta) = 2[\gamma_1^D\gamma_s^D]^{1/2} + 2[\gamma_1^P\gamma_s^P]^{1/2} \qquad (3)$$

where, γ_1, γ_s^P and γ_s^D are surface tension of test liquid, the polar component and the dispersive component of the surface free energy of the liquid and γ_s^{tot} is the total surface free energy, respectively. The values of the surface free energies of the test liquids obtained from the literature are given in **Table S1**. ([44]).

The *in vitro* release experiments were carried out in 50 mL of phosphate buffered saline solution (PBS, pH = 7.4, 0.9 wt.% NaCl content) at 37 °C. The MMC loaded 1 cm × 1 cm PVA based thin films with their rougher surface facing the outside were fixed to a 2.6 cm × 7.6 cm plastic foil. The samples were dried in an oven for 24 hours at 60 °C and subsequently placed into the gently stirred solution of PBS. At selected time intervals, 3 mL of release samples were withdrawn from the release media, and the determination of the released MMC concentration was carried out spectrophotometrically, on the basis of previously plotted calibration curve (absorbance maximum value of MMC = 364 nm).

The X-ray diffractograms of the powdered MMC and polymer coated MMC were recorded on a Philips X-ray diffractometer (XRD) with CuK_α (=0.1542 nm) as the radiation source at ambient temperature in the 2–70° (2Θ) range applying 0.02° (2Θ) step size.

3. Results and discussion

3.1. Structural and quantitative characterization of the BTS hydrophobized PVA

The initial water-soluble properties of the PVA were modified by silylation with BTS molecules to get hydrophobized biopolymer with reduced solubility and wettability. After this modification the initially well-water-soluble PVA polymer becomes hydrophobic and the BTS-PVA powder floated on the surface of the water without any wetting or dissolving (**Fig. 1.**).
FTIR measurements were performed for the characterization of the synthesized hydrophobic PVA (**Fig. 2.**). The main peaks of PVA have been observed at 3280, 2960, 2925, 1720, 1425, 1380, 1325, 1250, 1100 and 840 cm^{-1}. These peaks are assigned to the O–H stretching vibration of the hydroxyl group, CH_2 asymmetric stretching vibration, CH_2 symmetric stretching vibration, C=O carbonyl stretching vibration, C–H bending vibration of CH_2, C–H deformation vibration, CH_2 wagging vibration, C–O–C stretching vibration, C–O stretching of acetyl groups and C–C stretching vibration, respectively [45–48]. It can be seen that the peak of OH (~3280 cm^{-1}) of BTS-PVA was reduced due to the functionalization of the OH group of PVA by BTS.

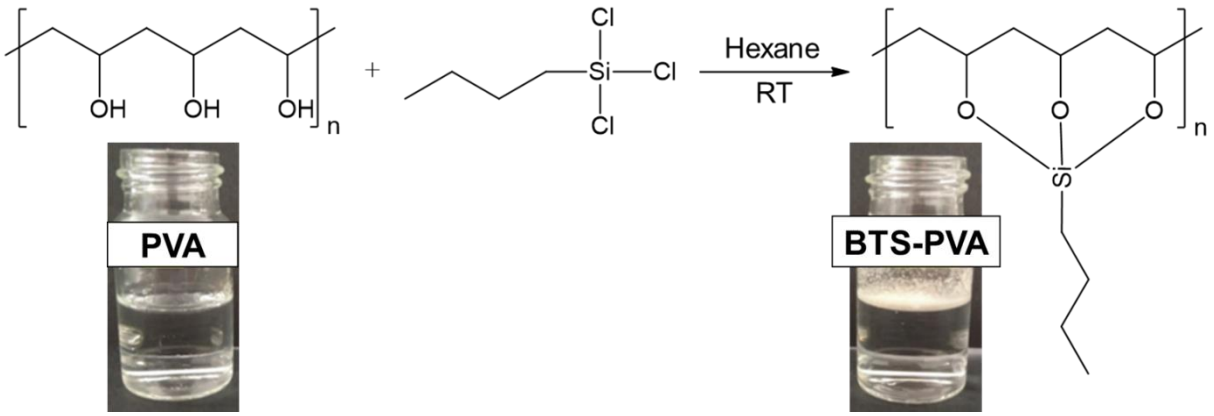

Figure 1. Silylation reaction of PVA using BTS molecules.

The main bands formed due to BTS treatment were observed at ~2880 cm^{-1} for terminal methyl groups of BTS and Si–O–C band at 1215 cm^{-1}. The formation of alkyl groups (C–CH_2) from BTS molecules was observed at 1463cm^{-1}. The new peak at 800 cm^{-1} was caused by stretching vibrations of the Si–O bonds that confirmed the successful reaction between BTS and the hydroxyl group of PVA [49,50].

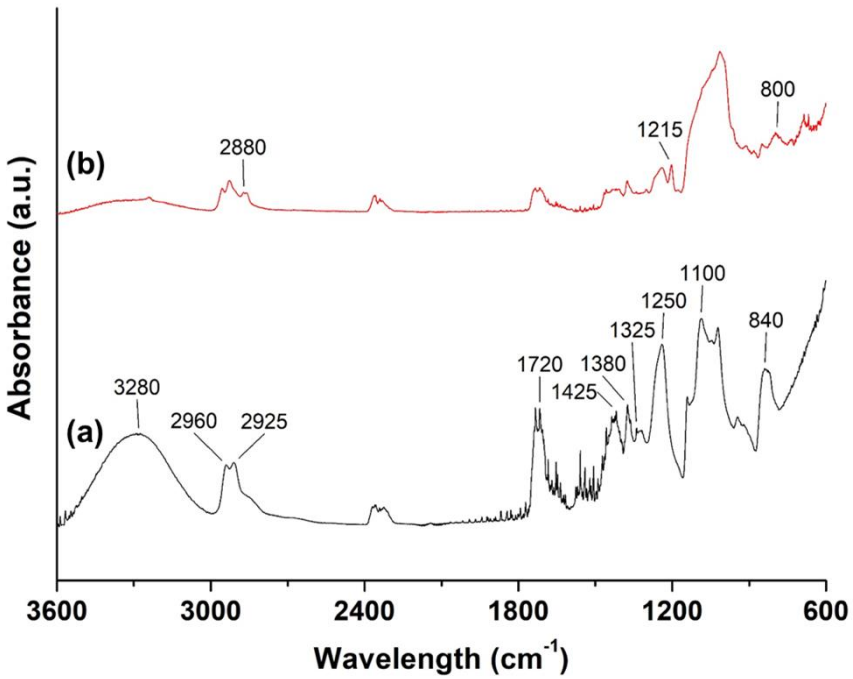

Figure 2. FTIR spectra of (a) initial PVA and (b) hydrophobized PVA (2 v/v% BTS).

The quantitative determination of OH value before and after the silylation was evaluated via an acetic anhydride/pyridine titration method. **Fig. 3.** shows the evolution of reacted OH groups with the increasing concentration of silylating agent (BTS) solution. The molar ratio of the reacted OH groups was calculated from the unreacted ones and the results reveal that increasing the concentration of BTS solution led to an increase in the reacted OH groups and at around 1 v/v% BTS solution it reached the saturation value with ~19% hydrophobization degree. The reason for this is that the PVA is insoluble in hexane and thus the modification of the polymer mainly occurred on the surface of PVA microparticles with a particle size of 10-20 μm (see the inserted microscopic image in **Fig. 3.**). However, it will be presented that this partial hydrophobization of the biopolymer is enough to prepare thin films even with superhydrophobic character.

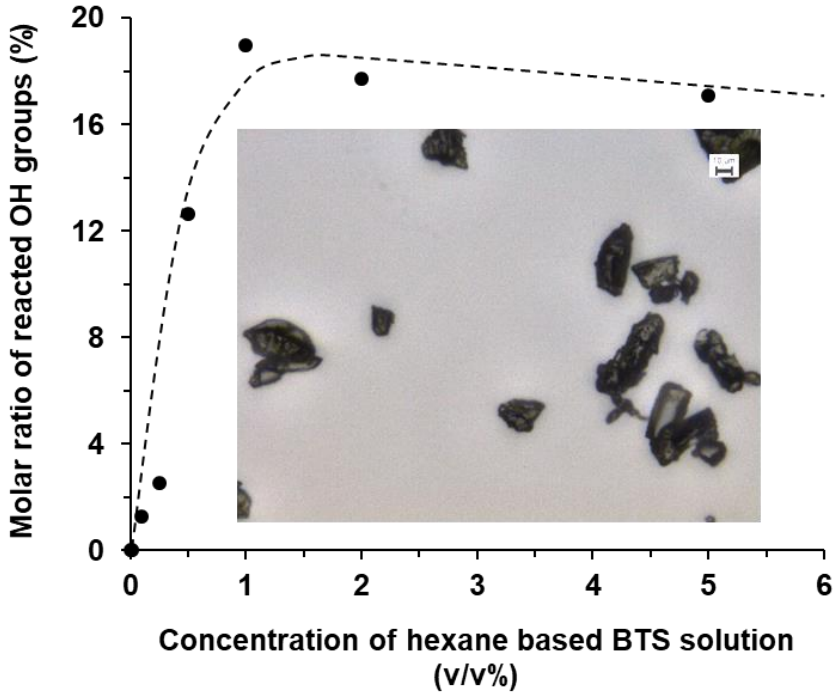

Figure 3. The effect of BTS solution concentration used during the PVA hydrophobization on the evolution of reacted OH groups. The dashed line is guide to eyes. The inserted photo shows the microscopic image of PVA particles (scale bar: 10 μm).

Based on the above presented results the 1% BTS-PVA sample was used for further experiments. After the structural characterization, the water-uptake properties of the samples were also examined in order to quantify the modified hydrophilicities of the samples. **Fig. 4.** shows the thermoanalytical (TG and DTA) curves of the initial PVA and the hydrophobically modified BTS-PVA. Before the TG measurements, the diluted 5 wt.% polymer solutions were concentrated by centrifugation, the supernatants were removed and the water contents of the obtained sediments were measured. The TG curves show that the weight loss of the initial PVA was significantly higher, the sample had 97.4 wt.% water content, while the BTS-PVA only contained 71.9 wt.% water. It can therefore be established that the hydrophobization of the PVA also manifests itself in the course of TG measurements and silylation of the polymer significantly reduced the water uptake properties of the PVA because the calculated values were 2.55 and 37.46 g water/g polymer for the BTS-PVA and unmodified PVA, respectively.

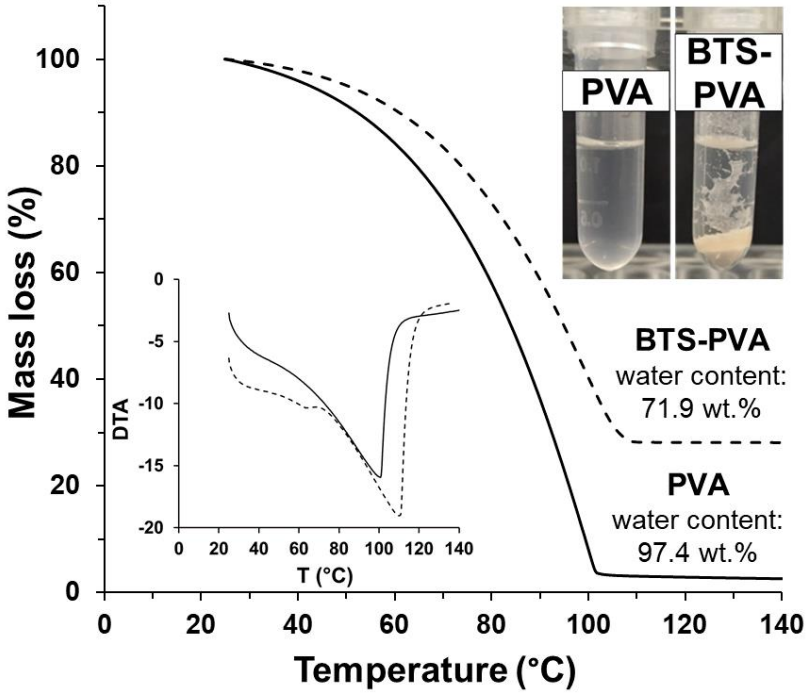

Figure 4. The TG and DTA (inserted figure) curves of the hydrophilic PVA and hydrophobic (1%) BTS-PVA based samples. The inserted picture represents the photos of the initial and hydrophobically modified PVA solution/dispersion in aqueous media before centrifugation (polymer content: 5 wt.%).

3.2 Morphological and wetting properties of the cellulose roughened and BTS hydrophobized PVA thin films

During the sample preparation water/ethanol (=90/10 v/v.%) mixture was used in order to increase the solubility of the MMC drug . Thus, the solubility of PVA, hydrophobized PVA and cellulose was also studied in water and in water/ethanol (=90/10 v/v.%) mixture (**Fig. S1**). The obtained results indicate that the initial PVA is soluble in water in a concentration of at least 15% but its solubility was continuously decreased with the increasing hydrophobicity and at 2% BTS silylated sample it was only 3.1% in water. However, in water/ethanol mixture the solubility of the hydrophobized samples was significantly higher and it can be seen that the obtained data exceeded the 10% during the whole range. The solubility of cellulose was also studied in both water and water/ethanol (=90/10 v/v.%) mixture and it was found that cellulose was practically insoluble in both media (0.7% in water and 1.02% in the mixture, respectively). According to the literature data cellulose is insoluble in water, partially soluble in ethanol [51] and thus the 90/10 v/v% water/ethanol mixture is suitable for dissolution of the MMC and PVA but not able to dissolve the cellulose particles.

After the hydrophobization of the PVA, the surface roughness of the thin films was adjusted by the incoroporation of cellulose microparticles. In the SEM images the initial, smooth (0 wt.% cellulose) hydrophilic PVA thin film and the hydrophilic and hydrophobic cellulose roughened thin films of different cellulose concentrations (60 and 90 wt%.) are presented at different magnifications (**Fig. 5.**). It can be observed that the initial, hydrophilic PVA thin film without cellulose content has a smooth surface, whereas in the case of the hydrophilic and superhydrophobic thin films, with the increasing – 60 and 90 wt%. – cellulose loading the surface roughness gradually increases.

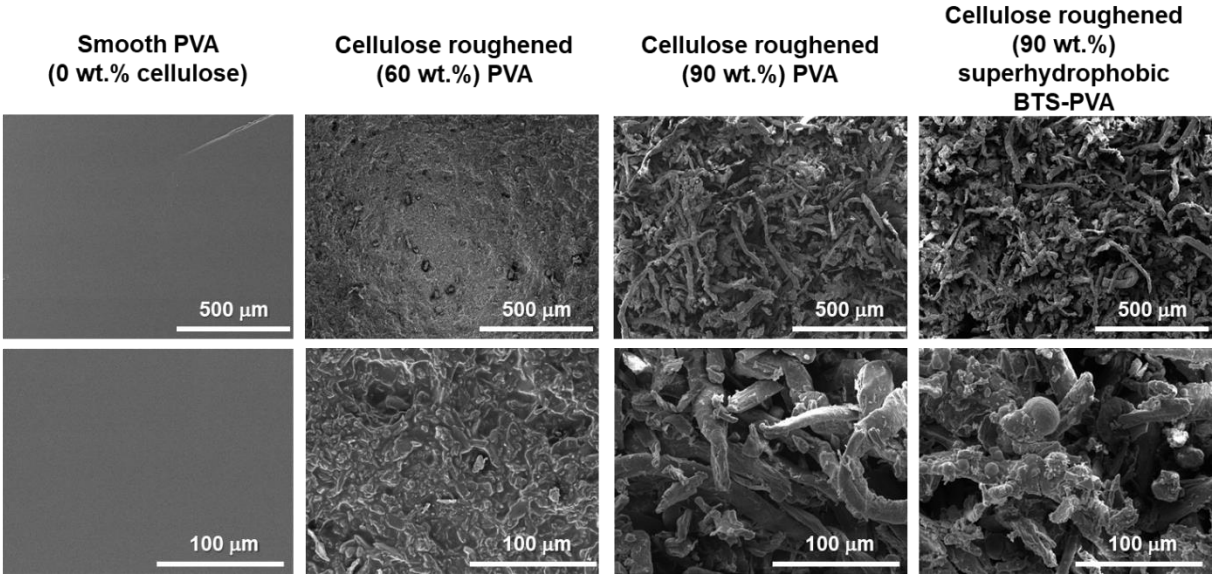

Figure 5. SEM images of the prepared smooth (0 wt.% cellulose), cellulose roughened (60 and 90 wt.%) hydrophilic PVA and cellulose roughened (90 wt.%) superhydrophobic BTS-PVA films.

The increase of the surface roughness with the increasing cellulose content observed in the SEM images was also confirmed by profilometry measurements (**Fig. 6.**). The R_a value measured on the initial hydrophilic, smooth (0 wt.% cellulose) PVA thin film was only 0.016±0.007 µm (**Fig. 6a.**), while the R_a values measured on the hydrophilic films with 60 and 90 wt.% cellulose were 12.15±0.47 (**Fig. 6b.**) and 31.57±4.77 µm (**Fig. 6c.**), respectively. The R_a value obtained in the case of cellulose roughened (90 wt.%) superhydrophobic BTS-PVA thin film was 26.64±1.20 µm (**Fig. 6d.**). It is worth to note that 15.61 % decrease in surface roughness was observed in the case of hydrophobic BTS-PVA (~26.64 µm) compared to the hydrophilic PVA (~31.57 µm) system at equal concentration of cellulose (90%) component incorporated. This is presumably because of the hydrophobic nature of both BTS-PVA and cellulose. Cellulose is a

water insoluble hydrophobic biopolymer and as a result, its compatibility with a hydrophilic (PVA) matrix is not as high as that with a hydrophobic (BTS-PVA) polymer. Thus, the incorporation of cellulose particles into hydrophilic PVA matrix resulted in a coarser, more inhomogeneous structure, which also caused rougher surface.

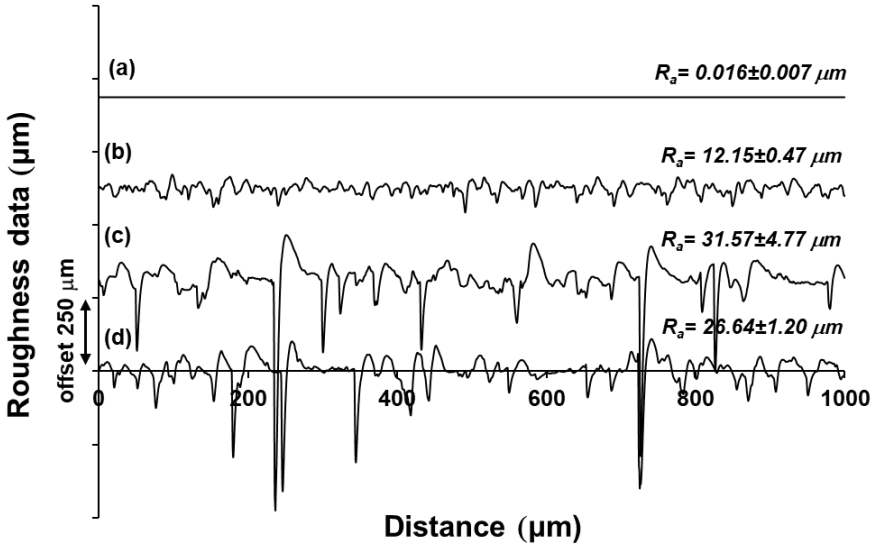

Figure 6. Measured profilometer data of the smooth (0 wt.% cellulose) hydrophilic PVA (a), cellulose roughened (60 wt.%) hydrophilic PVA (b), cellulose roughened (90 wt.%) hydrophilic PVA (c) and cellulose roughened (90 wt.%) superhydrophobic BTS-PVA (d) films with the profilometrically determined microscale surface roughness values (R_a).

The surface roughness values determined with profilometry measurements display the same trend which was observed in the SEM images: with the increasing cellulose concentration the surfaces roughness significantly increases.

In **Fig. S1** it was presented that the initial PVA and BTS hydrophobized PVA samples show different solubility in water and in 90/10 v/v% water/ethanol mixture. The hydrophobization of the PVA obviously decreased its water solubility but in water/ethanol mixture the BTS-PVA could be still dissolved. The preparation of the films occurred at 60 °C and at this temperature the faster evaporation of the ethanol and thus the enrichment of the water probably primarily caused the phase separation of the hydrophobic BTS-PVA rather than the hydrophilic PVA. This phase separation presumably caused inhomogeneities in the films but it is also worth to note that the porous structure and rough surface with high R_a values (**Fig. 6.**) were primarily caused by the incorporation of the cellulose particles rather than the phase separation of the PVA polymers.

The thickness of the PVA thin films having different surface roughness was measured with an Elcometer 224 type digital profile gauge. The obtained film thickness values varied between 60.8±5.5 and 206.6±10.2 µm, depending on their cellulose content (**Table 1.**).

The above presented results show that the incorporation of cellulose particles into the PVA matrix provided rough surface for the thin films. CT measurements were also performed in order to study the inner structure of the thin films. In **Fig. S2.** the representative 3D micro-CT images of flat (cellulose free) PVA (A) and 60% cellulose containing PVA (B) are presented. The difference is obviously: while the flat PVA film exhibited a dense and continuous layer (porosity: 0.7%), the 60 wt.% containing PVA film showed porous structure with a porosity of 64.9%). The porosity of the thin films were determined in all cases (**Table 1.**). The obtained results show that increasing cellulose content continuously increase the porosity of the thin films. However, it is also worth to note that the porous inner structure and rough surface of the hydrophobized films make the layers suitable for trapping air into the pores and in this way the water penetration is inhibited (**Fig. S5**) and thus the drug release can be prolonged (**Fig. 9** and **10**.).

In the following step, the effect of surface roughness on the wetting properties of the hydrophilic PVA and BTS hydrophobized PVA thin films with different cellulose loading was examined. According to the results presented above, adding cellulose to the polymer significantly affects the morphological properties, and thus the wettability of the film surfaces, which was confirmed by contact angle measurements (**Fig. 7.** and **Fig. 8.**). **Fig. 7.** shows the change in the contact angle values as a function of cellulose concentration of the thin films. In the case of the hydrophilic PVA thin films, the measured Θ values decreased (from Θ = 60.3° to Θ = 0°) with the increasing cellulose content (0–95 wt.%), the films became more and more (super)hydrophilic.

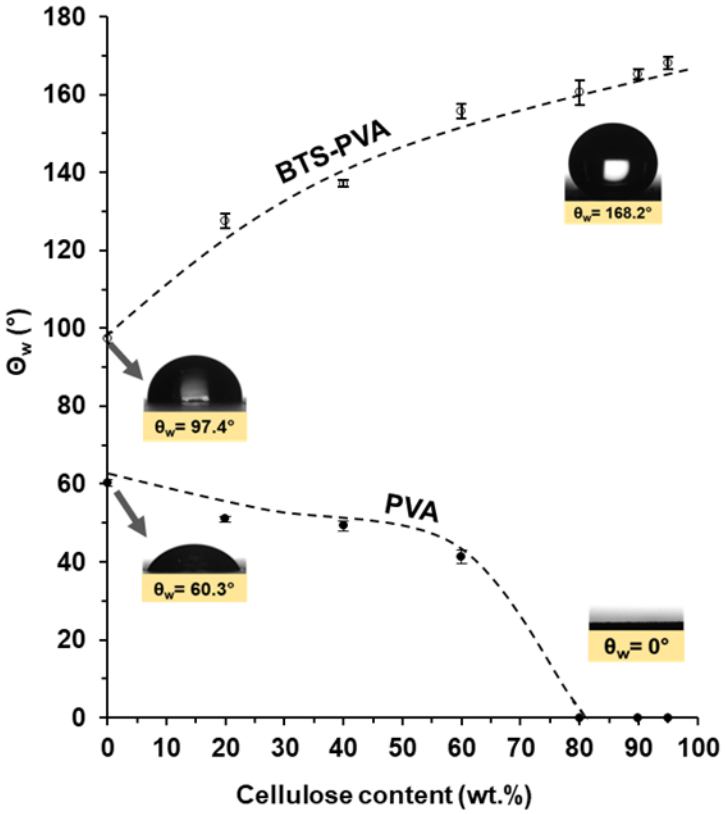

Figure 7. The measured static water contact angles (Θ_w) of the cellulose roughened hydrophilic PVA and 1% BTS hydrophobized PVA films.

For the BTS hydrophobized PVA thin films, it was found out that the increase of cellulose concentration, thus the increase of the surface roughness enhances the superhydrophobicity of the thin films (from $\Theta = 97.4°$ to $\Theta = 168.2°$). Thus, it can be seen that the roughness increases the wettability of wettable surfaces and decreases the unwettability of the unwettable ones.

The wettability of the smooth (0 wt.% cellulose) hydrophilic PVA and cellulose roughened (90 wt.%) superhydrophobic BTS-PVA thin films was also studied with dynamic contact angle measurements, the results of which are presented as a function of the drop volume in **Fig. 8**. The advancing (Θ_{adv}) and receding (Θ_{rec}) contact angles and the calculated γ_s^{tot} values were determined according to Drehlich's protocol [41]. In the case of the cellulose roughened (90 wt.%) superhydrophobic BTS-PVA thin film, the measured advancing contact angle (Θ_{adv}) values decreased from 160.2° to 159.2° as the drop volume was increased. However, with the decrease of the drop volume the receding (Θ_{rec}) contact angle values were significantly decreasing, from 159.2° to 75.5° (large contact angle hysteresis: $\Delta\Theta = 84.7°$). This value is considerably lower than that obtained during the static contact angle measurement ($\Theta = 165.3°$).

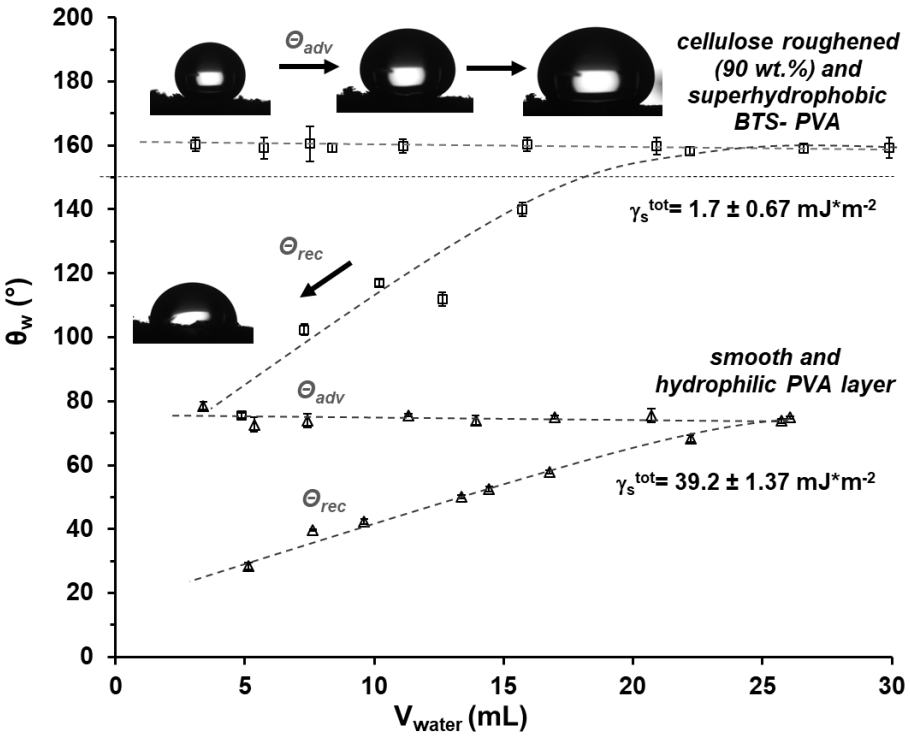

Figure 8. Evolution of advancing (Θ_{adv}) and receding (Θ_{rec}) water contact angles (Θ_w) as a function of water droplet volume (V_{water}) for the smooth (0 wt.% cellulose) hydrophilic PVA film and cellulose roughened (90 wt.%) superhydrophobic BTS-PVA layer (T= 25 °C ± 0.5 °C). The calculated surface free energy (γ_s^{tot}) values are added for both cases. The pictures of the liquid droplet on the hybrid layers are also shown.

The large contact angle hysteresis implies that the drop placed onto the cellulose roughened (90 wt.%) superhydrophobic BTS-PVA thin film is in the Wenzel state which may be caused by the wetting of the grooves on the cellulose roughened surface. The advancing (Θ_{adv}) contact angle values measured on the smooth (0 wt.% cellulose) hydrophilic PVA thin film slightly decreased with the increasing drop volume (from 78.5° to 74.9°), while the receding (Θ_{rec}) contact angle values were on a declining trend (from 74.9° to 28.4°) in this case, as well. The calculated γ_s^{tot} values were 39.2±1.37 and 1.7±0.67 mJ/m^2 for the smooth (0 wt.% cellulose) hydrophilic PVA and cellulose roughened (90 wt.%) superhydrophobic (90 wt.% cellulose) BTS-PVA thin films, respectively. Thus, it can be concluded that it is possible to prepare lotus-like superhydrophobic biopolymer thin films by roughening and functionalization of initial PVA.

The values of the total surface free energy (γ_s^{tot}) and its polar (γ_s^P) and dispersive (γ_s^D) components were also determined in the case of smooth (initial) PVA and the 60 wt.% cellulose containing hydrophilic and superhydrophobic samples according to Owens-Wendt-Kaelble equation (**Figure S3**). Since PVA is a relatively hydrophilic biopolymer, it has a relatively high

γ_s^{tot} value (39.7 ± 4.3 mJ/m^2) mainly with γ_s^P contribution (25.4 ± 3.2 mJ/m^2). Increasing the cellulose loading (and thus the roughness), the γ_s^{tot} and γ_s^P values were further increased to 52.6 ± 6.8 mJ/m^2 and 41.4 ± 3.9 mJ/m^2 (60 wt.% cellulose content). However, in the case of roughened and hydrophobized layer the γ_s^{tot} value drastically decreased to 1.9 ± 0.45 mJ/m^2 and its high γ_s^D content (1.7 ± 0.29 mJ/m^2) also indicates the hydrophobic surface characteristic.

3.3. Drug release experiments

In the previous sections it was shown how the different cellulose loadings affect the surface morphology and thus the wetting properties of the PVA thin films. In the following step, it was examined how this composition-controlled wetting property affects the release behaviour of the MMC loaded biopolymer thin films.

The release profiles of MMC released from the smooth (0 wt.% cellulose) and 59.85 wt.% cellulose roughened hydrophilic PVA, and from the smooth (0 wt.% cellulose) and 59.85 wt.% cellulose roughened superhydrophobic BTS-PVA thin films with different wettability are shown in **Fig. 9**. Each biopolymer based thin film contained the same amount of MMC drug (0.25 wt.%). To investigate the *in vitro* release behaviour of the free MMC, a control experiment was also conducted. Prior to the experiment, the free drug was enclosed in a cellulose membrane, then its release behaviour was studied in a stirred solution of PBS (pH = 7.4) at 37 °C. It was observed that after 1.5–2 h release time the fast, initial release rate of MMC (♦) gradually started to decrease. Namely, in the fast initial phase, 67.04% of the enclosed MMC was released from the cellulose membrane, whereas after 8 h only 79.61% of the initial drug load got released in the PBS medium. This is because of the moderate water solubility of the crystalline MMC. However, incorporation of the drug into the smooth (0 wt.% cellulose) hydrophilic PVA led to the increased release rate of MMC from the smooth PVA thin layers. The early phase of the drug dissolution from the smooth (0 wt.% cellulose) hydrophilic PVA thin films (■) consisted of a quick, initial release during which almost all amount of loaded drug (98.05%) was released (1 h). Roughening the surface of the hydrophilic PVA thin film with cellulose particles (59.85 wt.% cellulose) (♦) increased its wettability and facilitated the drug release from the biopolymer thin film: 98.08% of MMC was released in 0.5 h. In contrast, the hydrophobization of the thin films of different composition decreased the drug release rate. The smooth (0 wt.% cellulose) hydrophobic MMC/BTS-PVA thin film (●) released 99.93% of the incorporated drug load in 8 h, compared to the release rate of the smooth (0 wt.% cellulose)

hydrophilic biopolymer layers of the same composition (MMC/PVA). In the case of the cellulose roughened (59.85 wt.% cellulose) superhydrophobic MMC/BTS-PVA thin film (▲), the MMC release rate was even slower compared to the hydrophobic MMC/BTS-PVA thin film with smooth surface. Under 8 h release time, only 49.15% of the initial drug load was released from the film, whereas the smooth (0 wt.% cellulose) hydrophobic MMC/BTS-PVA layer released almost the whole amount of drug load (99.93%) for the same time. **Fig. 10.** shows the calculated appearent drug relase rate constant values (initial slopes of the curves, k') as a function of contact angles measured on the different surfaces.

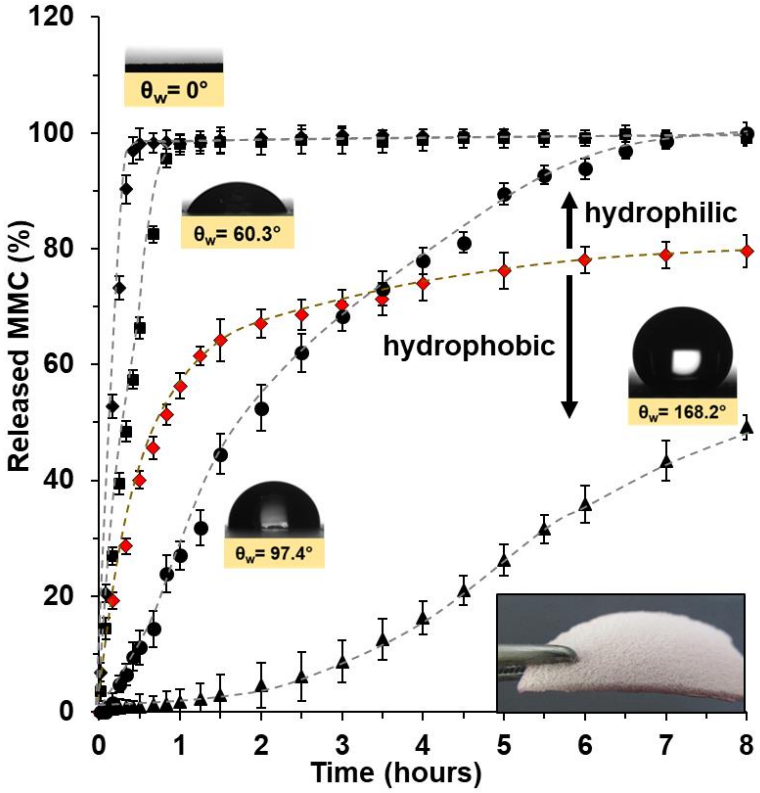

Figure 9. The percentage release profile of MMC molecules from the smooth (0 wt.% cellulose) hydrophilic PVA (■) and hydrophobic (●) BTS modified PVA films, 59.85 wt.% cellulose roughened hydrophilic (♦) and superhydrophobic BTS-PVA films (▲) as well as the release of bare MMC (♦) at pH=7.4 under physiological condition (0.9 wt.% NaCl content, 37 °C). The dashed lines are guide to eyes.

The dotted grey line represents the k' value (=1.21×10^{-6} mM/s) of the pure MMC. As it can be seen, incorporation of the MMC into the smooth (0 wt.% cellulose) hydrophilic (Θ= 60.3±0.83°) or cellulose roughened (59.85 wt.% cellulose) superhydrophilic (Θ= 0°) PVA films significantly increased the drug dissolution rate constants (2.07×10^{-6} and 6.1×10^{-6} mM/s, respectively). This is because of the lower crystallinity of the drug in PVA polymer matrix

which was also evidenced via XRD measurements (**Fig. 11.**). In the case of the MMC loaded smooth (0 wt.% cellulose) hydrophilic PVA sample the less sharper peaks indicated the partial amorphization of the drug in the polymer matrix which resulted in higher solubility and higher dissolution rate [30]. However, integrating MMC into the smooth (0 wt.% cellulose) hydrophobic (Θ= 97.4±1.44°) and cellulose roughened (59.85 wt.%) superhydrophobic (Θ= 165.3±1.36°) BTS-PVA samples significantly reduced the k' values (8×10^{-7} and 5×10^{-8} mM/s, respectively) (**Fig. 10.**). The above presented lower crystallinity and partial amorphization of the MMC in the polymer matrix were also verified via EDX measurements (**Fig. S4**). The nitrogen content of the MMC drug provides features for visualization of drug in the PVA based thin films. Without polymer matrix the bare MMC molecules formed well-developed micron-sized needle-like crystals during the precipitation/crystallization process (**Fig. S4 A.**). However, the SEM images and EDX represantations also show that in the presence of initial PVA (**Fig. S4 B.**) and cellulose containing hydrophobized PVA (**Fig. S4 C.**) well-defined spherical MMC micoparticles are formed. The corresponding XRD pattern of the MMC loaded samples shows lower intensity than the bare, uncoated MMC which corresponds to the lower crystallinity of the drug (**Fig. 11**). The lower crystallinity is advantageous, because the solubility of the drug molecules depends on the formation of intermolecular hydrogen bonds between the solvent and the solute molecules. The crystalline form is more stable than the amorphous form and has a lower energy at the molecular level with stronger bonding (mostly ionic bonds) between molecules that requires higher energy to break [26]. So, higher solubility means higher dissolution rate and better bioavailability.

Assuming that the MMC loaded cellulose roughened (59.85 wt.% cellulose) superhydrophobic BTS-PVA thin films display similar release behaviour *in vivo*, it could open a new pathway to design and develop antifibrotic drug delivery systems which are capable of targeted and/or prolonged MMC release. The release profiles of the released MMC from the thin films were affected in a great way by the film composition in every case. As the result of the hydrophobization of the cellulose roughened (59.85 wt.% cellulose) thin films, the rate of the MMC release significantly decreased.

In order to convince that really the surface wetting is the determining factor for the different release rates the wetting properties on the superhydrophobic layer (with 60% cellulose content) were studied as a function of time (**Fig. S5**). The presented contact angles measured over a long period of time indicate that after 3 h the film still shows superhydrophobic character because the measured values were above 150°. In **Fig. S4 C**. and **Fig. 11.** it was presented that in the polymer matrix the MMC forms microparticles with lower crystallinity, but even so the drug

release rate was significantly lower in the case of the superhydrophobic film (**Fig. 9.** and **10.**). This is obviously due to the strong water repellency and low water adhesion of the film. Moreover, upon immersion of the sample in water, an obvious mirror-like phenomenon could be observed (see graphical abstract when the superhydrophobic layer was immersed in aqueous medium) [52], which was mainly caused by the entrapped pocket of air at the sample surface-water interface.

Thus, it can be concluded that the incorporation of MMC into the polymer matrix resulted in lower drug crystallinity and partial amorphization and thus the drug release was faster from the well-wetting hydrophilic films compared to the pure MMC. However, in the case of the superhydrophobic film the drug release rate was significantly lower (**Fig. 9.** and **10.**). This is obviously due to the strong water repellency and low water adhesion of the film.

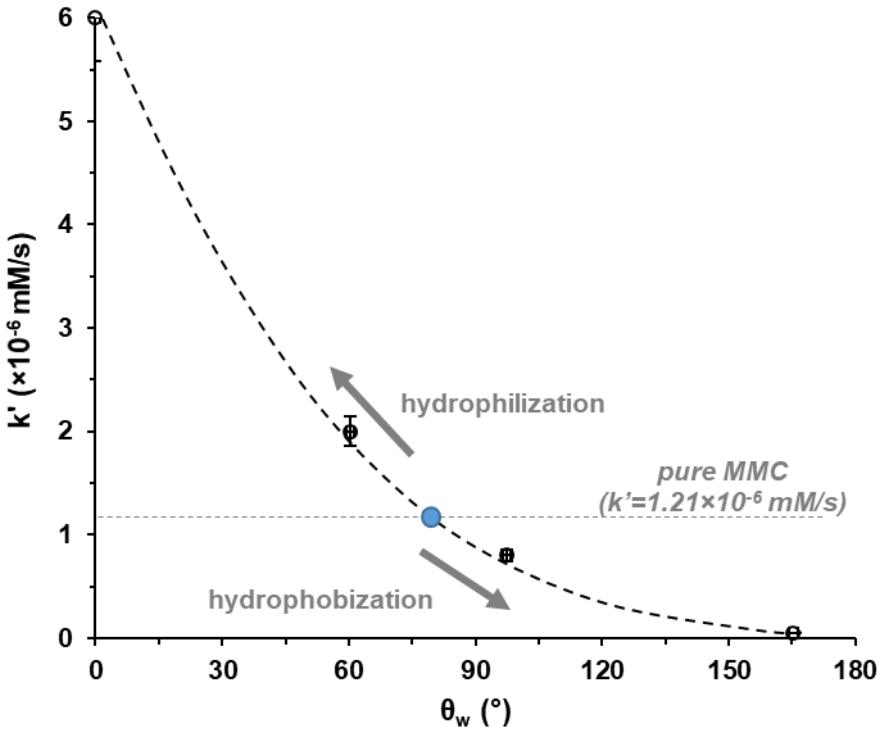

Figure 10. The effect of surface wetting properties on the the calculated appearent drug relase rate constant values (k').

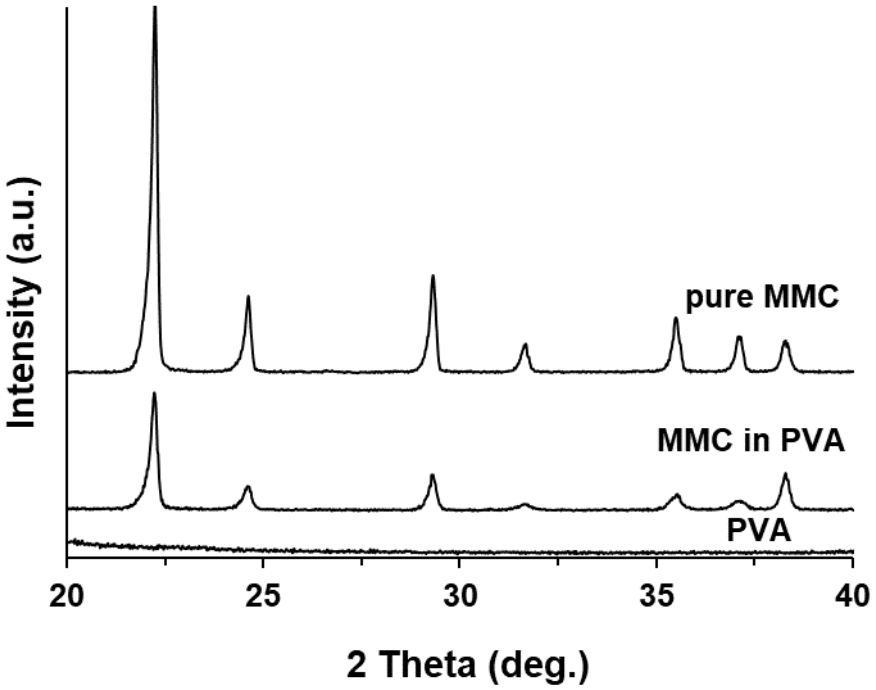

Figure 11. XRD patterns of the bare MMC drug microcrystals (a), the 10 wt.% MMC containing PVA thin film (b) and the smooth (0 wt.% cellulose) hydrophilic PVA thin film (c).

4. Conclusion

PVA based thin films were synthetised with systematically varied surface hydrophobicity and roughness and it was presented that the surface wetting was finely adjustable by these parameters from superhydrophilicity (Θ=0°) to superhydrophobicity (Θ=165.3°; γ_s^{tot} = 1.7±0.67 mJ/m^2). The successful silylation (hydrophobization) reaction of PVA by BTS molecules was confirmed by FTIR measurements. According to the results the ~19% hydrophobization degree of the initial PVA is sufficient to prepare thin films even with superhydrophobic character. The surface wetting was increased by the incorporation of cellulose microparticles into the smooth PVA films. As a result, the surface roughness increased from 0.016±0.007 µm (initial smooth PVA film) to 31.57±4.77 µm (90 wt.% cellulose containing hydrophilic PVA) and to 26.64±1.20 µm (90 wt.% cellulose containing hydrophobic PVA). Due to the non-wetting properties of the superhydrophobic BTS-PVA film, a trapped air layer forms on the surface of water-repellent materials in aqueous environment hindering water penetration. Consequently, because of the excellent isolation effect from the trapped surface air layer, the dissolution of the encapsulated MMC drug was strongly inhibited. The results showed that the drug release rate constant values (k') of antifibrotic MMC are well controllable by the surface wetting properties of the PVA thin films within a relatively wide dissolution range (from

$k'=6.1\times10^{-6}$ mM/s (superhydrophilic PVA film with 60 wt.% cellulose content) to $k'=5\times10^{-8}$ mM/s (superhydrophobic BTS-PVA film with 60 wt.% cellulose content). We propose that the presented biocompatible thin films loaded with antifibrotic MMC with obvious surface wetting driven release can be useful in the area of head and neck surgeries to prevent scar tissue formation.

Acknowledgements

The authors are very thankful for the financial support from the Hungarian Scientific Research Fund (OTKA) K 132446 and for the financial support from the project named GINOP-2.3.2-15-2016-00013. This paper was also supported by the UNKP-20-5 New National Excellence Program of the Ministry For Innovation and Technology and by the János Bolyai Research Scholarship of the Hungarian Academy of Sciences. The Ministry of Human Capacities, Hungary grant 20391-3/2018/FEKUSTRAT is also acknowledged. Á.K. acknowledges support from the Indo-Hungarian Joint Research project no. INT/HUN/P-18/2017 (NKFIH 2017- 2.3.7-TÉT-IN-2017-00008).

Declaration of Competing Interest

The authors declare that they have no known competing financial interests or personal relationships that could have appeared to influence the work reported in this paper.

Supplemental information

Supplemental Information can be found online at …

Data availability

All data used in the preparation of this manuscript is contained within this document.

References

[1] D. Szabó, D. Kovács, V. Endrész, N. Igaz, K. Jenovai, G. Spengler, L. Tiszlavicz, J. Molnár, K. Burián, M. Kiricsi, L. Rovó, Antifibrotic effect of mitomycin-C on human vocal cord fibroblasts, Laryngoscope. 129 (2019) E255–E262. https://doi.org/10.1002/lary.27657.

[2] I. Schipper, C. Suppelt, J.O. Gebbers, Mitomycin C reduces scar formation after excimer laser (193 nm) photorefractive keratectomy in rabbits, Eye. 11 (1997) 649–655. https://doi.org/10.1038/eye.1997.171.

[3] S.R. Merritt, G. Velasquez, H.A. von Recum, Adjustable release of mitomycin C for inhibition of scar tissue formation after filtration surgery, Exp. Eye Res. 116 (2013) 9–16. https://doi.org/10.1016/j.exer.2013.07.005.

[4] P.D. Karkos, S.C. Leong, A. Sastry, A.D. Assimakopoulos, A.C. Swift, Evidence-based applications of mitomycin C in the nose, Am. J. Otolaryngol. - Head Neck Med. Surg. 32 (2011) 422–425. https://doi.org/10.1016/j.amjoto.2010.07.022.

[5] M.L. Ubell, S.L. Ettema, R.J. Toohill, C.B. Simpson, A.L. Merati, Mitomycin-c application in airway stenosis surgery: Analysis of safety and costs, Otolaryngol. - Head Neck Surg. 134 (2006) 403–406. https://doi.org/10.1016/j.otohns.2005.10.057.

[6] A.L. Myers, Y.P. Zhang, J.D. Kawedia, X. Zhou, S.M. Sobocinski, M.J. Metcalfe, M.A. Kramer, C.P.N. Dinney, A.M. Kamat, Solubilization and Stability of Mitomycin C Solutions Prepared for Intravesical Administration, Drugs R D. 17 (2017) 297–304. https://doi.org/10.1007/s40268-017-0183-y.

[7] A. Martin, Martin's physical pharmacy and pharmaceutical sciences : physical chemical and biopharmaceutical principles in the pharmaceutical sciences., Lippincott Williams & Wilkins, Baltimore MD, 2011.

[8] A. Takada, S.L. Nail, M. Yonese, Subambient behavior of mannitol in ethanol-water co-solvent system, Pharm. Res. 26 (2009) 568–576. https://doi.org/10.1007/s11095-008-9775-0.

[9] P.J. Gandhi, Z.V.P. Murthy, Measurement of solubility of mitomycin C in ethanol-water solutions at different temperatures, Thermochim. Acta. 545 (2012) 163–173. https://doi.org/10.1016/j.tca.2012.07.014.

[10] Y. Haque, E.; Kikuchi, T.; Kanemitsu, K.; Tsuda, NII-Electronic Library Service, Chem. Pharm. Bull. 34 (1986) 430–433.

[11] L.K. Fung, W.M. Saltzman, Polymeric implants for cancer chemotherapy, Adv. Drug

Deliv. Rev. 26 (1997) 209–230. https://doi.org/10.1016/S0169-409X(97)00036-7.

[12] Y. Ikeuchi-Takahashi, C. Ishihara, H. Onishi, Evaluation of polyvinyl alcohols as mucoadhesive polymers for mucoadhesive buccal tablets prepared by direct compression, Drug Dev. Ind. Pharm. 43 (2017) 1489–1500. https://doi.org/10.1080/03639045.2017.1321657.

[13] N.A. Peppas, N.K. Mongia, Ultrapure poly(vinyl alcohol) hydrogels with mucoadhesive drug delivery characteristics, Eur. J. Pharm. Biopharm. 43 (1997) 51–58. https://doi.org/10.1016/S0939-6411(96)00010-0.

[14] B. Chaudhuri, B. Mondal, S.K. Ray, S.C. Sarkar, A novel biocompatible conducting polyvinyl alcohol (PVA)-polyvinylpyrrolidone (PVP)-hydroxyapatite (HAP) composite scaffolds for probable biological application, Colloids Surfaces B Biointerfaces. 143 (2016) 71–80. https://doi.org/10.1016/j.colsurfb.2016.03.027.

[15] M.H.A. Zanin, N.N.P. Cerize, A.M. de Oliveira, Production of Nanofibers by Electrospinning Technology: Overview and Application in Cosmetics, Nanocosmetics and Nanomedicines. (2011) 311–332. https://doi.org/10.1007/978-3-642-19792-5_16.

[16] L. V. Thomas, U. Arun, S. Remya, P.D. Nair, A biodegradable and biocompatible PVA-citric acid polyester with potential applications as matrix for vascular tissue engineering, J. Mater. Sci. Mater. Med. 20 (2009) 259–269. https://doi.org/10.1007/s10856-008-3599-7.

[17] G. Leone, M. Consumi, G. Greco, C. Bonechi, S. Lamponi, C. Rossi, A. Magnani, A PVA/PVP hydrogel for human lens substitution: Synthesis, rheological characterization, and in vitro biocompatibility, J. Biomed. Mater. Res. - Part B Appl. Biomater. 97 B (2011) 278–288. https://doi.org/10.1002/jbm.b.31813.

[18] P. Picone, M.A. Sabatino, A. Ajovalasit, D. Giacomazza, C. Dispenza, M. Di Carlo, Biocompatibility, hemocompatibility and antimicrobial properties of xyloglucan-based hydrogel film for wound healing application, Int. J. Biol. Macromol. 121 (2019) 784–795. https://doi.org/10.1016/j.ijbiomac.2018.10.078.

[19] E. Yan, Y. Fan, Z. Sun, J. Gao, X. Hao, S. Pei, C. Wang, L. Sun, D. Zhang, Biocompatible core-shell electrospun nanofibers as potential application for chemotherapy against ovary cancer, Mater. Sci. Eng. C. 41 (2014) 217–223. https://doi.org/10.1016/j.msec.2014.04.053.

[20] E.A. Kamoun, E.R.S. Kenawy, T.M. Tamer, M.A. El-Meligy, M.S. Mohy Eldin, Poly (vinyl alcohol)-alginate physically crosslinked hydrogel membranes for wound dressing applications: Characterization and bio-evaluation, Arab. J. Chem. 8 (2015) 38–47.

https://doi.org/10.1016/j.arabjc.2013.12.003.

[21] T. Noguchi, T. Yamamuro, M. Oka, P. Kumar, Y. Kotoura, S. Hyon, Y. Ikada, Poly(vinyl alcohol) hydrogel as an artificial articular cartilage: evaluation of biocompatibility., J. Appl. Biomater. 2 (1991) 101–107. https://doi.org/10.1002/jab.770020205.

[22] I. Manavi-Tehrani, M. Rabiee, M. Parviz, M.R. Tahriri, Z. Fahimi, Preparation, characterization and controlled release investigation of biocompatible pH-sensitive PVA/PAA hydrogels, Macromol. Symp. 296 (2010) 457–465. https://doi.org/10.1002/masy.201051062.

[23] W.J. Sherwood, S. D. Atmurr, Patent Application Publication (10) Pub . No .: US 2005 / 0131113 A1, 1 (2005) 6–9.

[24] W.S. Lee, M. Park, M.H. Kim, C.G. Park, B.K. Huh, H.K. Seok, Y. Bin Choy, Nanoparticle coating on the silane-modified surface of magnesium for local drug delivery and controlled corrosion, J. Biomater. Appl. 30 (2016) 651–661. https://doi.org/10.1177/0885328215582110.

[25] S.S. Laxmeshwar, D.J. Madhu Kumar, S. Viveka, G.K. Nagaraja, Preparation and Properties of Biodegradable Film Composites Using Modified Cellulose Fibre-Reinforced with PVA, ISRN Polym. Sci. 2012 (2012) 1–8. https://doi.org/10.5402/2012/154314.

[26] H. Ullah, H.A. Santos, T. Khan, Applications of bacterial cellulose in food, cosmetics and drug delivery, Cellulose. 23 (2016) 2291–2314. https://doi.org/10.1007/s10570-016-0986-y.

[27] J. Shokri, K. Adibki, Application of Cellulose and Cellulose Derivatives in Pharmaceutical Industries, Cellul. - Medical, Pharm. Electron. Appl. (2013). https://doi.org/10.5772/55178.

[28] B.A. Kakade, V.K. Pillai, Tuning the wetting properties of multiwalled carbon nanotubes by surface functionalization, J. Phys. Chem. C. 112 (2008) 3183–3186. https://doi.org/10.1021/jp711657f.

[29] E. Celia, T. Darmanin, E. Taffin de Givenchy, S. Amigoni, F. Guittard, Recent advances in designing superhydrophobic surfaces, J. Colloid Interface Sci. 402 (2013) 1–18. https://doi.org/10.1016/j.jcis.2013.03.041.

[30] L. Janovák, Á. Turcsányi, É. Bozó, Á. Deák, L. Mérai, D. Sebők, Á. Juhász, E. Csapó, M.M. Abdelghafour, E. Farkas, I. Dékány, F. Bari, Preparation of novel tissue acidosis-responsive chitosan drug nanoparticles: Characterization and in vitro release properties of Ca2+ channel blocker nimodipine drug molecules, Eur. J. Pharm. Sci. 123 (2018) 79–

88. https://doi.org/10.1016/j.ejps.2018.07.031.

[31] E. Csapó, Juhász, N. Varga, D. Sebők, V. Hornok, L. Janovák, I. Dékány, Thermodynamic and kinetic characterization of pH-dependent interactions between bovine serum albumin and ibuprofen in 2D and 3D systems, Colloids Surfaces A Physicochem. Eng. Asp. 504 (2016) 471–478. https://doi.org/10.1016/j.colsurfa.2016.05.090.

[32] W. Barthlott, C. Neinhuis, Purity of the sacred lotus, or escape from contamination in biological surfaces, Planta. 202 (1997) 1–8. https://doi.org/10.1007/s004250050096.

[33] H.K. Webb, R.J. Crawford, E.P. Ivanova, Wettability of natural superhydrophobic surfaces, Adv. Colloid Interface Sci. 210 (2014) 58–64. https://doi.org/10.1016/j.cis.2014.01.020.

[34] M. Ma, R.M. Hill, Superhydrophobic surfaces, Curr. Opin. Colloid Interface Sci. 11 (2006) 193–202. https://doi.org/10.1016/j.cocis.2006.06.002.

[35] I. Yilgor, S. Bilgin, M. Isik, E. Yilgor, Tunable wetting of polymer surfaces, Langmuir. 28 (2012) 14808–14814. https://doi.org/10.1021/la303180k.

[36] N.J. Shirtcliffe, G. McHale, M.I. Newton, The superhydrophobicity of polymer surfaces: Recent developments, J. Polym. Sci. Part B Polym. Phys. 49 (2011) 1203–1217. https://doi.org/10.1002/polb.22286.

[37] R.N. Wenzel, Resistance of solid surfaces to wetting by water, Ind. Eng. Chem. 28 (1936) 988–994. https://doi.org/10.1021/ie50320a024.

[38] B.D. Cassie, A.B.D. Cassie, S. Baxter, Of porous surfaces, Trans. Faraday Soc. 40 (1944) 546–551. https://doi.org/10.1039/tf9444000546.

[39] R. Fürstner, W. Barthlott, C. Neinhuis, P. Walzel, Wetting and self-cleaning properties of artificial superhydrophobic surfaces, Langmuir. 21 (2005) 956–961. https://doi.org/10.1021/la0401011.

[40] J.D. Miller, S. Veeramasuneni, J. Drelich, M.R. Yalamanchili, G. Yamauchi, Effect of roughness as determined by atomic force microscopy on the wetting properties of PTFE thin films, Polym. Eng. Sci. 36 (1996) 1849–1855. https://doi.org/10.1002/pen.10580.

[41] J. Drelich, Guidelines to measurements of reproducible contact angles using a sessile-drop technique, Surf. Innov. 1 (2013) 248–254. https://doi.org/10.1680/si.13.00010.

[42] E. Chibowski, Surface free energy of a solid from contact angle hysteresis, Adv. Colloid Interface Sci. 103 (2003) 149–172. https://doi.org/10.1016/S0001-8686(02)00093-3.

[43] D.K. Owens, R.C. Wendt, Estimation of the surface free energy of polymers, J. Appl. Polym. Sci. 13 (1969) 1741–1747. https://doi.org/10.1002/app.1969.070130815.

[44] I. Torchinsky, G. Rosenman, Wettability modification of nanomaterials by low-energy electron flux, Nanoscale Res. Lett. 4 (2009) 1209–1217. https://doi.org/10.1007/s11671-009-9380-0.

[45] N. V. Bhat, M.M. Nate, M.B. Kurup, V.A. Bambole, S. Sabharwal, Effect of γ-radiation on the structure and morphology of polyvinyl alcohol films, Nucl. Instruments Methods Phys. Res. Sect. B Beam Interact. with Mater. Atoms. 237 (2005) 585–592. https://doi.org/10.1016/j.nimb.2005.04.058.

[46] J. Lee, T. Isobe, M. Senna, Preparation of ultrafine Fe3O4 particles by precipitation in the presence of PVA at high pH, J. Colloid Interface Sci. 177 (1996) 490–494. https://doi.org/10.1006/jcis.1996.0062.

[47] I. Omkaram, R.P. Sreekanth Chakradhar, J. Lakshmana Rao, EPR, optical, infrared and Raman studies of VO2+ ions in polyvinylalcohol films, Phys. B Condens. Matter. 388 (2007) 318–325. https://doi.org/10.1016/j.physb.2006.06.134.

[48] A. Kharazmi, N. Faraji, R.M. Hussin, E. Saion, W.M.M. Yunus, K. Behzad, Structural, optical, opto-thermal and thermal properties of ZnS-PVA nanofluids synthesized through a radiolytic approach, Beilstein J. Nanotechnol. 6 (2015) 529–536. https://doi.org/10.3762/bjnano.6.55.

[49] F. Yaghoubidoust, E. Salimi, Antibacterial and Antiplatelet Properties of Octyltrichlorosilane-modified Cotton Fabrics, Fibers Polym. 20 (2019) 1375–1379. https://doi.org/10.1007/s12221-019-1111-2.

[50] A. Kumar, J. Richter, J. Tywoniak, P. Hajek, S. Adamopoulos, U. Šegedin, M. Petric, Surface modification of Norway spruce wood by octadecyltrichlorosilane (OTS) nanosol by dipping and water vapour diffusion properties of the OTS-modified wood, Holzforschung. 72 (2017) 45–56. https://doi.org/10.1515/hf-2017-0087.

[51] S. Naz, N. Ahmad, J. Akhtar, N.M. Ahmad, A. Ali, M. Zia, Management of citrus waste by switching in the production of nanocellulose, IET Nanobiotechnology. 10 (2016) 395–399. https://doi.org/10.1049/iet-nbt.2015.0116.

[52] L. Shen, W. Qiu, B. Liu, Q. Guo, Stable superhydrophobic surface based on silicone combustion product, RSC Adv. 4 (2014) 56259–56262. https://doi.org/10.1039/c4ra10838h.

Declaration of interests

☒ The authors declare that they have no known competing financial interests or personal relationships that could have appeared to influence the work reported in this paper.

☐The authors declare the following financial interests/personal relationships which may be considered as potential competing interests:

Author contributions:

Tamás Takács: Investigation, Validation, original draft preparation

Mohamed M. Abdelghafour: Investigation, Validation, original draft preparation

Ágota Deák: Investigation, Writing - Review & Editing

Diána Szabó: Investigation, Writing - Original Draft

Dániel Sebők: Investigation, Writing - Review & Editing

Imre Dékány: Writing - Review & Editing

László Rovó: Writing - Review & Editing

Ákos Kukovecz: Supervision, Conceptualization, original draft preparation

László Janovák: Supervision, Conceptualization, methodology, original draft preparation